CHEMMEDCHEM
Chemistry & Drug Discovery

Supporting Information

Development of Small-Molecule Cryptochrome Stabilizer Derivatives as Modulators of the Circadian Clock

Jae Wook Lee,[a, c] Tsuyoshi Hirota,*[b, d, e] Anupriya Kumar,*[b, f] Nam-Jung Kim,[a, g] Stephan Irle,[b, f] and Steve A. Kay*[b, d]

cmdc_201500260_sm_miscellaneous_information.pdf

SI Methods

A. Biological assays

Cell-based circadian assay

The assay was performed as described previously[1]. Stable U2OS reporter cells harboring *Bmal1-dLuc* or *Per2-dLuc* were suspended in the culture medium [DMEM (11995-073, Gibco) supplemented with 10% fetal bovine serum, 0.29 mg/mL L-glutamine, 100 units/ml penicillin, and 100 μg/mL streptomycin] and plated onto 384-well white solid-bottom plates at 20 μL (2,000 cells) per well. After 2 days, 50 μL of the explant medium [DMEM (12800-017, Gibco) supplemented with 2% B27 (Gibco), 10 mM HEPES, 0.38 mg/mL sodium bicarbonate, 0.29 mg/mL L-glutamine, 100 units/mL penicillin, 100 μg/mL streptomycin, and 1 mM luciferin, pH7.2] was dispensed to each well, followed by the application of 500 nL of compounds (dissolved in DMSO). The plate was covered with an optically clear film and set to a microplate reader (Infinite M200, Tecan). The luminescence was recorded every 100 min for 5 days. The period parameter was obtained from the luminescence rhythm by curve fitting program MultiCycle (Actimetrics). The luminescence intensity parameter was calculated by averaging the intensity during the experiment. The first day data were excluded from the analysis because of transient luminescence changes upon the medium change.

Protein degradation assay

The assay was performed as described previously[1]. Stable HEK293 cells harboring CRY1-LUC or LUC reporter were suspended in the culture medium and plated onto 384-well white solid-bottom plates at 50 μL (1.0×10^4 cells) per well. After 24h, 500 nl of the compound was added to the medium. After 24 h, the medium was supplemented with luciferin (final 1 mM) and HEPES-NaOH (pH7.2; final 10 mM). After 1 h, cycloheximide (final 20 μg/ml) was added, and the luminescence was recorded every 10 min for 18 h with Infinite M200. Half-life was obtained by one phase exponential decay fitting with Prism software (GraphPad Software).

B. 3D-QSAR study

Structure preparation and docking

The molecular structures of the compounds were prepared by using the Torch[2] software by adding hydrogen atoms and minimizing the structures using a XED[3] force field. The DockPrep module of UCSF Chimera[4] was used to prepare the CRY protein structure bound to KL001 (PDB X-ray structure 4MLP[5]) by adding the missing side chains using the Dunbrack[6] rotamer library, adding hydrogens and Gasteiger charges using ANTECHAMBER[7]. To prepare the protein and the ligand structures for docking, PDBQT files were generated using AutoDock Tools 1.5.6[8]. Default values were applied for all the docking parameters. The size of the docking grid was 40 Å × 40 Å × 40 Å. KL044 was docked in the CRY protein using the Lamarckian Genetic Algorithm method in AutoDock 4.2[8]. As a check, using this methodology, the crystal structure binding pose of KL001 was reproduced. For visualization of the best docking pose, UCSF Chimera's ViewDock module was used.

Pharmacophore generation by FieldTemplater

In FieldTemplater[9], 500 low energy ligand conformations were used for the conformational search of the template molecules. Parameters such as the maximum number of conformations were set to 500, the number of high-T dynamics runs for flexible rings was set to 10, the gradient cutoff for conformer minimization was set to 0.30 kcal/mol/Å, and the RMS value to filter duplicate conformers was set to 0.50 Å. For template building, the minimum number of molecules per template was set to 2, the maximum number of comparisons per pair was set to 200, the maximum score delta per pair was set to 0.1, the minimum link density in a template was set to 0.8, and duplicate templates were filtered at 0.7 Å. For the conformational search, yielding an optimal alignment to the template, the score fraction from the shape similarity was set to 0.5, a weighted average score method was used for multiple reference. No field constrains were applied for building the template.

For representing electrostatic and van der Waals properties of ligands (**figure 2A**), field points[10] were derived using the XED[3] force field by calculating the Coulombic interaction between probe atoms such as a charged oxygen atom for positive (red) and negative field points (cyan). A neutral oxygen atom was used as probe for calculating the Morse potential term for van der Waals interactions (yellow). Neutral oxygen atoms were also used to calculate the attractive energy term for hydrophobic field points (orange) by assigning zero weights to the electronegative atoms. The size of the field points in **figure 2A** corresponds to the magnitude of the interaction energy. This employs molecular field based similarity methods for conformational search to design a pharmacophore template which resembles the bioactive conformation. The two compounds used for the pharmacophore template generation were KL001 (PDB crystal structure 4MLP) and KL044 docked into the crystal structure of CRY protein bound to KL001. The pharmacophore was obtained by the conformational search of KL001 and KL044 in FieldTemplater[9], which resembles their respective bioactive conformation in CRY protein. In the pharmacophore template based on low energy conformations of KL001 and KL044, the values for 2D-similarity, field similarity and shape similarity were 0.763, 0.699 and 0.827, respectively. As previously shown, in the case of Cholecystokinin 2 Receptor Antagonists[11] and novel reversible Cdc25 inhibitors[12], ligand field point profiles for structurally different ligands were related to their binding capability in the protein. Hence, ligand fields essential for binding could be elucidated and used for virtual screening.

3D-QSAR based on the field points

The pharmacophore template obtained from the FieldTemplater[9] was directly transferred into the Forge[9] software, where the compounds were aligned to the template. Field point based descriptors were used for building 3D-QSAR model after the alignment of 60 compounds on to the pharmacophore template. For building the 3D-QSAR model, the maximum number of components was set to 20, the sample point maximum distance was set to 1.0 Å, Y scrambles were set to 50, and Electrostatic as well as Volume fields were used. For overall similarity, Forge uses 50% Field similarity and 50% Dice volume similarity. The overlays with the best matching low energy conformation to the template were taken into consideration for building the 3D-QSAR model. Linear correlation between similarity and field similarity with the experimental pEC_{50}s were obtained from the alignment of the compounds to the pharmacophore template as shown in **figure S2A** and **S2B**. This provided a good starting point for building a 3D-QSAR model.

Generation of prediction set and field pattern contribution to the predicted activity

Design principal for KL065 is described in the main text and **figure 3B**, and that for KL066, KL067, KL068, and KL069 is described below. Their activities are listed in **table S1**.

To obtain a compound with favorable sterics, mesyl group in KL034 was modified to carbonyl t-butyl in KL066 to have better activity as shown by cyan cubes in **figure S4A**. Other substitutions such as phenyl moiety in KL037 and cyclo-propane in KL036 increase the unfavorable sterics (purple cubes).

To study whether the hydrogen bond of –OH with S394 can be replaced with halogen interaction, –OH moiety in KL001 was modified to di-fluoro moiety in KL067, which resulted in lowering of the activity. The replacement of mesyl group with octanal (KL068) or 3-cyclopropyl-1H-pyrazole (KL069) also resulted in the lowering of the activity indicating the importance of CH-π interactions with W290 and W397. The bulkier replacements of mesyl moiety were sterically hindered.

Based on the field pattern contribution to the predicted activity, **figure S4B** shows the evolution of medicinal chemistry for ortho substituent at benzyl moiety that supports the benefit of ortho modification indicated in **figure 4A**. When the –F moiety (KL047) is substituted to -CF_3 (KL048) or –I (KL043) moiety, the activity increases due to the improved electrostatics (cyan cubes) while increasing the unfavorable sterics (purple cubes).

C. Chemical synthesis

General. All chemicals and solvents were obtained from commercial suppliers (Acros and Aldrich) and used without further purification. Unless otherwise indicated, all reactions were run under argon gas. Anhydrous solvents were purchased from Acros chemical company. ^{1}H and ^{13}C NMR spectra were recorded on a Bruker 400 MHz spectrometer. Chemical shifts are reported relative to internal $CDCl_3$ (Me_4Si, δ 0.0) and CD_3CN (Me_4Si, δ 0.0). All compounds were identified by LC-MS from Agilent Technology, using a C_{18} column (20 × 4.0 mm), with 20 minutes elution using a gradient solution of CH_3CN-H_2O (containing 0.05% trifluoroacetic acid), with UV detector and an electrospray ionization source.

General procedure of the synthesis of compound 3.

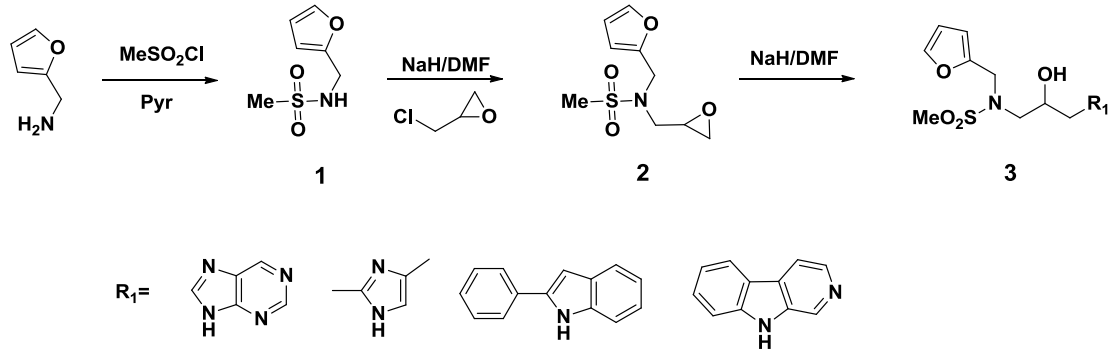

Scheme S1. The scheme of a synthesis of compound **3**.

The synthesis of N-(furan-2-ylmethyl)methanesulfonamide (1). A solution of furfuyl amine (500 mg, 5.15 mmol) in pyridine (4 mL) was treated with methansulforyl chloride (500 uL, 6.17 mmol). The reaction mixture was stirred for 24h at room temperature. The reaction mixture was diluted with CH_2Cl_2, washed with 5% HCl solution, and brine. The organic layer was dried over Na_2SO_4, filtered, and concentrated under reduced pressure. The crude compound was purified by flash column chromatography (CH_2Cl_2:Hexane=1:1) to give a grey color solid (767.6 mg, 85.3%)

The synthesis of N-(furan-2-ylmethyl)-N-(oxiran-2-ylmethyl)methanesulfonamide (2). A solution of compound **1** (500 mg, 2.85mmol) in DMF (10 mL) was treated with NaH (85 mg, 3.42mmol, 1.2 equiv) at 0 ^oC, stirring for 1 hr at 0 ^oC and treated with epibromohydrine (465 mg, 3.42mmol). The reaction mixture was stirred overnight at 50 ^oC. The reaction mixture was diluted with CH_2Cl_2, washed with 5% HCl solution, and brine. The organic layer was dried over Na_2SO_4, filtered, and concentrated under reduced pressure. The crude compound was purified by flash column chromatography (CH_2Cl_2:Hexane=1:2) to give a solid (343 mg, 52.1%)

The synthesis of compounds (3). A solution of carbazole (50 mg, 0.21mmol) in DMF (3 mL) was treated with NaH (11 mg, 0.42mmol, 2.0 equiv) and stirred for 30min at room temperature, followed by compound 2 (48 mg, 0.2 mmol) in DMF (2 mL). The reaction mixture was stirred for 2 hrs at 60 ^oC. The reaction mixture was diluted with ethyl acetate, washed with 5% HCl, and brine. The crude material was purified by flash column chromatography to give compounds.

KL007

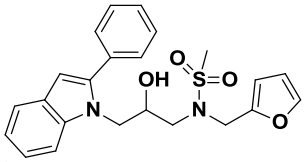

^{1}H NMR (**$CDCl_3$-*d*, 400 MHz**) δ ; 7.64 (d, J=8Hz, 1H), 7.50-7.48(m, 4H), 7.48-7.39(m, 3H), 7.29 (dd, J=1.6, 0.8 Hz, 1H), 7.25 (m, 1H), 7.15 (t, J=7.2 Hz, 1H), 6.56 (d, J=0.4Hz, 1H), 6.24 (dd, J=3.2, 2 Hz, 1H), 5.95 (d, J=3.2, 1H), 4.38-4.22 (m, 4H), 4.13 (d, J=16.4 Hz, 1H), 4.05 (br s, 1H), 3.02 (dd, J=14.8, 8 Hz, 1H), 2.88 (dd, J=14.8, 3.6 Hz, 1H), 2.7 (s, 3H).
ESI-MS: 425.1 (M+H), 447.1 (M+Na).

KL009

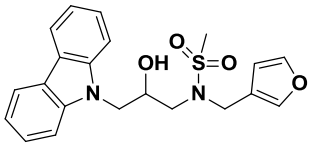

^{1}H NMR (**$CDCl_3$-*d*, 400 MHz**) δ ; 8.09 (d, J=8 Hz, 2H), 7.46 (t, J=8.0, 8.4 Hz, 2H), 7.36 (d, J=8.4Hz, 2H), 7.27-7.23 (m, 3H), 7.01 (d, J=0.4 Hz, 1H), 6.21 (d, J=1.6, 0.8 Hz), 4.37-4.21 (m. 3H), 4.23 (d, J=15.2 Hz, 1H), 4.11 (d, J=15.2 Hz, 1H), 3.42-3.27 (m, 1H), 3.20-3.16 (m, 1H), 2.81 (s, 3H).

General procedure for the synthesis of compound 7.

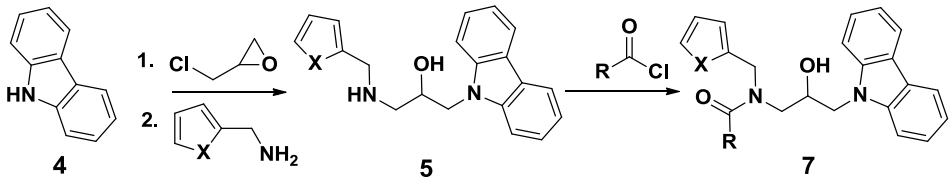

Scheme S2. The scheme of the synthesis of compound **7**.

We followed the previous procedure[1] for the synthesis of compound **5**. A solution of 1-(9H-carbazol-9-yl)-3-((furan-2-ylmethyl)amino)propan-2-ol (**5**) (50 mg, 0.16mmol) in THF (2 mL) was treated with DIEA (20 mg, 0.16mmol, 25 mL) and followed acyl chloride (0.16 mmol). After stirring at room temperature overnight, the reaction mixture was extracted with ethyl acetate (50 mL) and water (20 mL). Organic layer was dried with $MgSO_4$. The organic layer was evaporated under reduced pressure. Crude compound was purified by Prep-HPLC with 0.05 % trifluoroacetic acid-water/0.05 % trifluoroacetic acid- acetonitrile to afford compound.

KL011

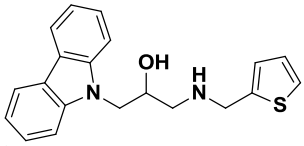

^{1}H NMR (**MeOD-*d*, 400 MHz**) δ ; 8.16 (d, J=8Hz, 2H), 7.61 (d, J=8.5Hz, 2H),7.54-7.51 (m, 3H), 7.30 (t, J=8Hz, 2H), 7.17 (d, J=3Hz, 1H), 7.07 (dd, J=5, 3.5 Hz, 1H), 4.54-4.46 (m, 5H), 3.17 (dd, J=12.5, 10 Hz, 1H), 3.10 (dd, J=12.5, 2.5 Hz, 1H).
^{13}C NMR (**MeOD-*d*, 100 MHz**) δ ; 140.98, 131.12, 128.59, 127.66, 127.64, 127.46, 125.95, 123.38, 120.20, 119.45, 109.13, 101.79, 66.07, 49.50, 48.0, 46.0.
ESI-MS : 337.1 (M+H).

KL012

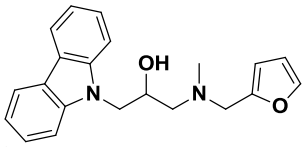

^{1}H NMR (**$CDCl_3$-*d*, 400 MHz**) δ ; 8.11 (d, J=8.0 Hz, 2H), 7.55-7.45 (m, 4H), 7.34 (d, J=1.6 Hz, 1H), 7.26 (d, J=8.0 Hz, 2H), 6.30 (dd, J=3.2, 2.0 Hz, 1H), 6.12 (d, J=3.2 Hz, 1H), 4.36 (d, J=5.6 Hz, 2H), 4.23-4.17 (m, 1H), 3.59 (d, J=3.6 Hz, 2H), 2.57 (t, J=9.6 Hz, 1H), 2.46 (dd, J=12.4, 4 Hz, 1H), 2.27 (s, 3H).

KL013

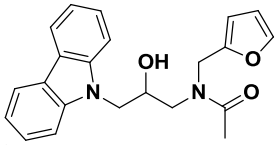

^{1}H NMR (**$CDCl_3$-*d*, 400 MHz**) δ ; 8.10 (d, J=7.6Hz, 2H), 7.45 (t, J=8, 2H), 7.39 (d, J=8, 2H), 7.24 (t, J=7.6Hz, 2H), 7.07 (dd, J=2, 0.8Hz, 1H), 5.97 (dd, J=3.2, 1.6Hz, 1H), 5.55 (dd, J=3.2, 0.4Hz, 1H), 4.46 (br s, 1H), 4.36-4.21 (m, 2H), 4.17-4.10 (m, 3H), 3.79 (dd, J=14.4, 8.8Hz, 1H), 3.17 (dd, J=14.4, 2Hz, 1H), 2.23 (s, 3H).
^{13}C NMR (**$CDCl_3$-*d*, 100 MHz**) δ ; 173.38, 148.81, 142.73, 140.58, 125.87, 122.99, 120.31, 119.23, 110.18, 109.00, 108.60, 71.00, 52.28, 47.41, 47.04, 21.72.
ESI-MS : 363.1 (M+H), 385.1 (M+Na).

KL014

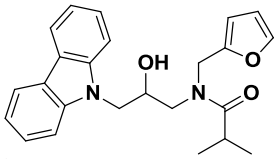

^{1}H NMR (**$CDCl_3$-*d*, 400 MHz**) δ ; 8.02 (d, J=7.6 Hz, 2H), 7.50-7.35 (m, 5H), 7.24-7.20 (m, 2H), 6.28 (d, J=3.2 Hz, 1H), 6.25 (dd, J=3.2, 2 Hz, 1H), 4.54-4.43 (m, 2H), 4.07 (s, 2H), 3.24 (d, J=7.2 Hz, 1H), 3.11 (dd, J=13.2, 8 Hz, 1H), 2.34 (ddd, J=21.2, 14.0, 7.2 Hz, 1H), 1.16 (dd, J= 14.8, 6.8 Hz, 1H), 0.9 (d, J=6.8 Hz, 3H), 0.76 (d, J=6.8 Hz, 3H).
ESI-MS : 392.2 (M+H).

KL016

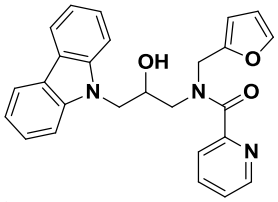

^{1}H NMR (**$CDCl_3$-*d*, 400 MHz**) δ ; 8.03 (d, J=7.6 Hz, 2H), 7.65-7.62 (m, 2H), 7.50-7.38 (m, 5H), 7.24-7.19 (m, 3H), 7.05-7.01 (m, 1H), 6.22 (dd, J=3.2, 2.0 Hz, 1H), 6.11 (d, J=2.8 Hz, 1H), 5.13 (d, J=15.2 Hz, 1H), 4.58-4.49 (m, 2H), 4.38-4.27 (m, 2H), 3.52 (dd, J=14.8, 12.0 Hz, 1H), 3.19 (dd, J=15.2, 3.2 Hz, 1H).
^{13}C NMR ($CDCl_3$-*d*, 100 MHz) δ ; 167.8, 151.9, 149.9, 145.7, 142.4, 141.1, 138.0, 125.7, 125.5, 124.9, 122.9, 120.1, 119.1, 110.5, 109.5, 109.4, 68.0, 50.6, 47.5, 41.5.
ESI-MS : 426.2 (M+H), 448.2 (M+Na).

KL018

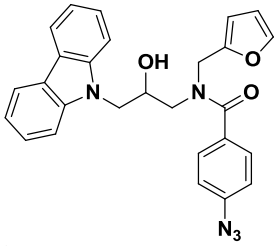

^{1}H-NMR (**$CDCl_3$-*d*, 400 MHz**) δ ; 8.10 (d, J=7.6 Hz, 2H), 7.56 (s, 2H), 7.5-7.35 (m, 4H), 7.25 (m, 3H), 7.06 (s, 2H), 5.88 (s, 1H), 5.35 (s, 1H), 4.45-4.25 (m, 2H), 4.25-4.10 (m, 3H), 3.95 (m, 1H), 3.30-3.22 (m, 1H).
ESI-MS : 466.2 (M+H), 488.2 (M+Na).

KL019

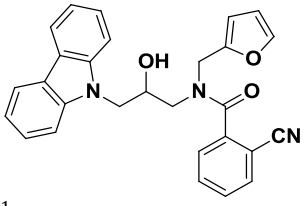

^{1}H-NMR (**$CDCl_3$-*d*, 400 MHz**) δ ; 8.10 (d, J=8.0 Hz, 2H), 7.65 (d, J=8.0 Hz, 2H), 7.62 (d, J=8 Hz, 2H), 7.47-7.37 (m, 4H), 7.28-7.23 (m, 2H), 7.13 (s, 1H), 5.95 (s, 1H), 5.46 (s, 1H), 4.41-4.23 (m, 3H), 4.17-4.08 (m, 2H), 3.89 (dd, J=14, 8.4Hz, 1H), 3.36 (d, J=14.4 Hz, 1H).
^{13}C NMR ($CDCl_3$-*d*, 100 MHz) δ ; 171.9, 149.0, 147.7, 144.5, 143.1, 140.5, 139.5, 132.5, 128.0, 126.2, 126.0, 123.0, 120.4, 119.3, 114.0, 110.3, 109.7, 108.9, 70.5, 51.2, 47.7, 47.1.
ESI-MS : 450.2 (M+H), 472.1 (M+Na).

General procedure for the synthesis of compound 10.

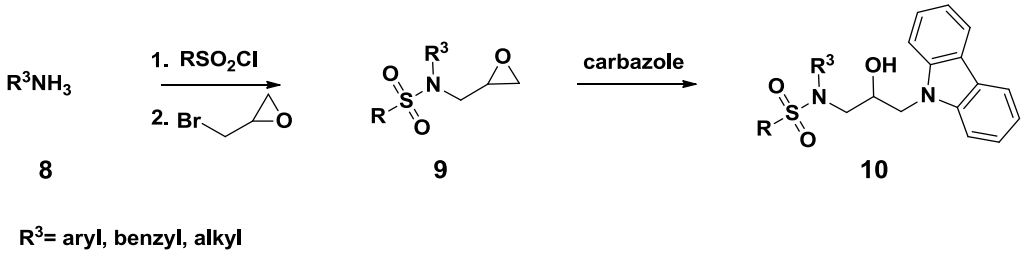

Scheme S3. The scheme of the synthesis of compound **10**.

We followed the previous procedure for the synthesis of compound **9**. A solution of carbazole (250 mg, 1.5mmol) in DMF (5 mL) was treated with NaH (41 mg, 1.7mmol, 1.2 equiv) and stirred for 30min at room temperature, followed by compound **9** (242 mg, 0.85mmol) in DMF (2 mL). The reaction mixture was stirred for 2 hrs at 60 ^{o}C. The reaction mixture was diluted with ethyl acetate, washed with 5% HCl, and brine. The crude material was purified by flash column chromatography to give compounds.

KL021

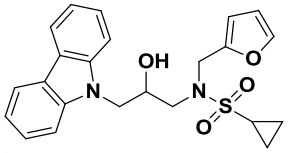

^{1}H-NMR (**$CDCl_3$-*d*, 400 MHz**) δ ; 8.09 (d, J=7.6Hz, 2H), 7.46 (t, J=8 Hz, 2H), 7.41 (d, J=7.6Hz, 2H), 7.25 (t, J=8Hz, 2H), 7.17 (dd, J=1.6, 0.8Hz, 1H), 6.13 (dd, J=3.2, 1.6Hz, 1H), 5.93 (d, J=3.2Hz, 1H), 4.40-4.31 (m, 4H), 4.27-4.22 (m, 1H), 3.47 (dd, J=14.8, 8Hz, 1H), 3.28 (dd, J=14.8, 3.2Hz, 1H), 2.28 (m, 1H), 1.63-1.12 (m, 2H), 0.93-0.89 (m, 2H).
^{13}C NMR (**$CDCl_3$-*d*, 100 MHz**) δ ; 149.19, 142.86, 140.62, 125.89, 123.05, 120.34, 119.32, 110.46, 110. 09, 108.97, 69.22, 51.55, 46.83, 45.20, 28.97, 5.24, 4.97.
ESI-MS : 425.1 (M+H), 447.1 (M+Na).

KL022

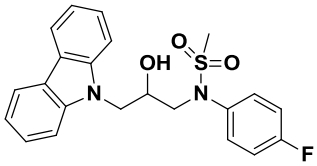

^{1}H NMR (**$CDCl_3$-*d*, 400 MHz**) δ ; 8.07 (d, J=7.6Hz, 2H), 7.44 (t, J=8.4Hz, 2H), 7.37-7.31 (m, 4H), 7.24 (t, J=8Hz, 2H), 7.07 (t, J=8Hz, 2H), 4.45-4.34 (m, 2H), 4.32-4.25 (m, 1H), 3.92 (dd, J=14.4, 7.6Hz, 1H), 3.76 (dd, J=14.4, 4.8Hz, 1H), 2.91 (s, 3H).
^{13}C NMR (**$CDCl_3$-*d*, 100 MHz**) δ ; 140.65, 130.38, 130.29, 125.95, 123.09, 120.39, 119.46, 116.85, 116.62, 108.83, 69.11, 55.17, 37.43.
ESI-MS : 413.1 (M+H), 435.1 (M+Na).

KL024

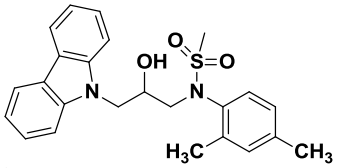

^{1}H NMR (**$CDCl_3$-*d*, 400 MHz**) δ ; 8.06 (d, J=7.6 Hz, 2H), 7.42 (t, J=7.6 Hz, 2H), 7.35 (t, J=8 Hz, 2H), 7.23 (t, J=7.6 Hz, 2H), 7.13-7.03 (m, 2H), 6.99-6.95 (m, 1H), 4.37-4.25 (m, 3H), ?
ESI-MS : 423.1 (M+H), 445.1 (M+Na).

KL025

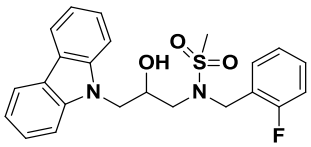

^{1}H NMR (**$CDCl_3$-*d*, 400 MHz**) δ ; 8.11 (d, J=7.6 Hz, 2H), 7.44 (td, J=8.4, 1.2 Hz, 2H), 7.32 (d, J=8Hz, 2H), 7.27-7.22 (m, 2H), 7.23-7.10 (m, 2H), 6.93 (td, J=7.2, 0.8 Hz, 1H), 6.90-6.86 (m, 1H), 4.49 (d, J=14.8 Hz, 1H), 4.35 (d, J=14.8 Hz, 1H), 4.30-4.21 (m, 3H), 3.5 (m, 1H), 3.22 (m, 1H). 2.89 (s, 3H). ^{13}C NMR (**$CDCl_3$-*d*, 100 MHz**) δ ;

ESI-MS : 427.1 (M+H), 449.1 (M+Na).

KL026

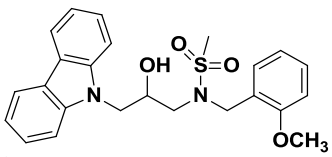

^{1}H NMR (**$CDCl_3$-*d*, 400 MHz**) δ ; 8.10 (d, J=7.6Hz, 2H), 7.44 (t, J=7.8Hz, 2H), 7.32 (d, J=8.0Hz, 2H), 7.24 (t, J=7.4 Hz, 2H), 7.16-7.10 (m, 2H), 6.75 (t, J=7.4 Hz, 1H), 6.21 (d, J=8.4 Hz, 1H), 4.41 (d, J=14.4 Hz, 1H), 4.32-4.18 (m, 4H), 3.43 (m, 1H), 3.42 (s, 3H), 3.28 (m, 1H), 2.81 (s, 3H).
^{13}C NMR (**$CDCl_3$-*d*, 100 MHz**) δ ; 157.3, 140.6, 131.4, 129.7, 125.9, 123.0, 122.9, 120.8, 120.3, 119.3, 110.6, 108.9, 68.9, 54.9, 51.9, 47.1, 47.0, 38.4.
ESI-MS : 439.2 (M+H), 461.1 (M+Na).

KL027

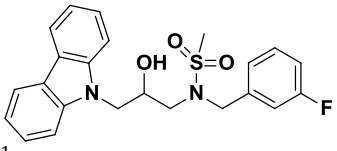

^{1}H NMR (**$CDCl_3$-*d*, 400 MHz**) 8.08 (d, J=7.6Hz, 2H), 7.43 (t, J=8.4 Hz, 2H), 7.27 (d, J=8Hz, 2H), 7.24 (t, J=8Hz, 2H), 7.08 (m,1H), 6.86 (m, 2H), 6.79 (m, 1H), 4.32 (d, J=14.8, 1H), 4.27-4.16 (m, 4H), 3.46 (dd, J=15.2, 8Hz, 1H), 3.16 (dd, J=15.2, 2.4Hz, 1H), 2.9 (s, 3H).
^{13}C NMR (**$CDCl_3$-*d*, 100 MHz**) δ ; 164.1, 161.6, 140.43, 137.90, 137.83, 130.38, 130.29, 125.96, 124.01, 123.97, 123.03, 120.41, 119.43, 115.48, 115.28, 115.26, 115.07, 108.74, 68.73, 52.07, 51.68, 46.96, 38.69.
ESI-MS : 427.1 (M+H), 449.1 (M+Na).

KL028

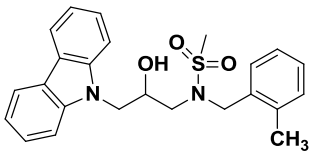

^{1}H NMR (**$CDCl_3$-*d*, 400 MHz**) δ ; 8.07 (d, J=8.4 Hz, 2H), 7.47 (td, J=8.4, 1.2 Hz, 2H), 7.24-7.18 (m, 4H), 7.06-6.99 (m, 2H), 6.93 (d, J=7.2 Hz, 1H), 6.87-6.83 (m, 1H), 4.45 (d, J=13.6 Hz, 1H), 4.19-4.04 (m, 3H), 3.86 (m, 1H), 3.45 (dd, J=15.2, 8.8 Hz, 1H), 3.15 (dd, J=18, 3.2 Hz, 1H), 2.94 (s, 3H), 2.21 (s, 3H).
^{13}C NMR (**$CDCl_3$-*d*, 400 MHz**) δ ; 140.5, 137.2, 132.5, 130.9, 129.5, 128.4, 126.1, 125.8, 123.0, 120.3, 119.3, 108.8, 69.0, 52.1, 51.4, 46.9, 41.0, 37.1, 19.0
ESI-MS : 423.1 (M+H), 445.1 (M+Na).

KL029

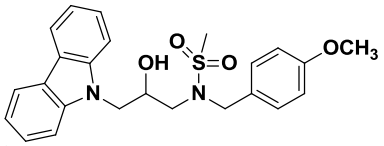

^{1}H-NMR (**$CDCl_3$-*d*, 400 MHz**) 8.11 (d, J=7.2 Hz, 2H), 7.44 (t, J=7.2 Hz, 2H), 7.29-7.23 (m, 4H), 6.92 (d, J=8.8 Hz, 2H), 6.65 (d, J=8.4 Hz, 2H), 4.28-4.13 (m, 5H), 3.76 (s, 3H), 3.44 (dd, J=14.8, 8 Hz, 1H), 3.16 (dd, J=15.2, 2.8 Hz, 1H), 2.86 (s, 3H).

KL032

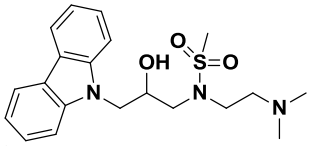

^{1}H-NMR (**$CDCl_3$-*d*, 400 MHz**) δ ; 8.05 (d, J=7.6 Hz, 2H), 7.50 (d, J=8 Hz, 2H), 7.45 (t, J=8.0 Hz, 2H), 7.22 (t, J=8.0Hz, 2H), 4.45-4.34 (m, 3H), 3.70-3.65 (m, 1H), 3.53-3.46 (m, 1H), 3.42-3.28 (m, 2H), 3.24-3.11 (m, 2H), 2.78 (s, 3H), 2.74 (m, 6H).
ESI-MS : 390.2 (M+H).

KL033

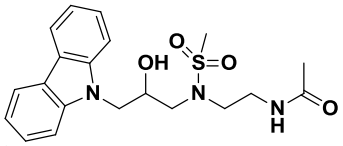

^{1}H NMR (**$CDCl_3$-*d*, 400 MHz**) δ ; 8.06 (d, J=7.6 Hz, 2H), 7.5-7.43 (m, 4H), 7.28-7.20 (m, 2H), 6.33 (s, 1H), 4.48-4.38 (m, 1H), 4.3 (t, J=6 Hz, 2H), 3.45-3.35 (m, 2H), 3.35-3.20 (m, 3H), 3.18-3.10 (m, 1H), 2.79 (s, 3H), 1.87 (s, 3H).
^{13}C NMR (**$CDCl_3$-*d*, 100 MHz**) δ ; 171.3, 140.8, 126.0, 123.0, 120.3, 119.4, 109.1, 69.6, 54.3, 49.4, 47.3, 38.7, 37.1, 23.1.
ESI-MS : 404.2 (M+H), 426.1 (M+Na).

KL034

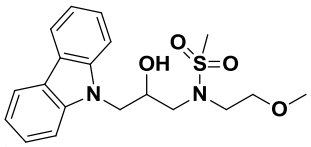

^{1}H-NMR (**$CDCl_3$-*d*, 400 MHz**) δ ; 8.09 (d, J=7.6Hz, 2H), 7.49-7.46 (m, 4H), 7.27-7.22 (m, 2H), 4.43-4.32 (m, 3H), 3.83 (d, J=3.6Hz, 1H), 3.5-3.47 (m, 2H), 3.45-3.28 (m, 5H), 3.23 (s, 3H), 2.85 (s, 3H).
^{13}C NMR (**$CDCl_3$-*d*, 100 MHz**) δ ; 140.83, 125.87, 123.05, 120.33, 119.28, 109.04, 71.40, 69.82, 58.79, 53.90, 49.47, 37.74.
ESI-MS : 377.1 (M+H), 399.1 (M+Na).

KL036

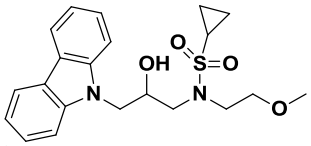

^{1}H-NMR (**$CDCl_3$-*d*, 400 MHz**) δ ; 8,11 (d, J=7.6 Hz, , 2H), 7.51-7.46 (m, 4H), 7.28-7.24 (m, 2H), 4.46-4.32 (m, 3H), 3.55-3.51 (m, 2H), 3.49 (s, 1H), 3.47-3.42 (m, 2H), 3.38-3.32 (m, 2H), 3.27 (s, 3H), 2.27 (m, 1H), 1.038 (m, 2H), 0.86 (m, 2H).
ESI-MS : 403.1 (M+H), 425.1 (M+Na).

KL037

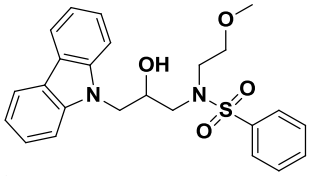

^{1}H-NMR (**$CDCl_3$-*d*, 400 MHz**) δ ; 8.10 (d, J=7.6 Hz, 2H), 7.56-7.54 (m, 2H), 7.51 (m, 1H), 7.47-7.46 (m, 4H), 7.4-7.36 (m, 2H), 7.28-7.24 (m, 2H), 4.44-4.40 (m, 2H), 4.35-4.29 (m, 1H), 3.58-3.54 (m, 2H), 3.38-3.28 (m, 2H), 3.26 (s, 3H), 3.17-3.04 (m, 2H).
ESI-MS : 439.1 (M+H), 461.1 (M+Na).

KL039

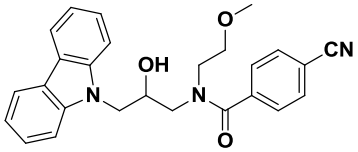

^{1}H-NMR (**$CDCl_3$-*d*, 400 MHz**) δ ; 8.16 (d, J=7.6 Hz, 2H), 7.43 (t, J=7.6 Hz, 2H), 7.28 (t, J=8.0 Hz, 2H), 7.26 (d, J=8 Hz, 2H), 6.85 (d, J=8 Hz, 2H), 6.71 (d, J=8.4Hz, 2H), 5.4 (s, 1H), 4.57-4.15 (m, 3H), 3.93-3.87 (m, 2H), 3.79-3.75 (m, 1H), 3.67-3.60 (m, 1H), 3.51 (s, 3H), 3.25-3.14 (m, 2H).
ESI-MS : 428.2 (M+H), 450.2 (M+Na).

The general procedure of the synthesis of compound 13.

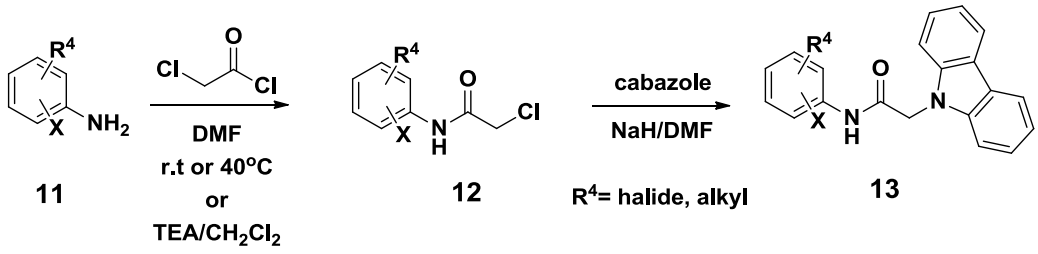

Scheme S4. The scheme of the synthesis of compound **13**.

Method A: A solution of compound **11** (100 mg, 1.1mmol) in DMF (5 mL) was treated with chloroacetyl chloride (102 μL, 1.2 mmol). The reaction mixture was stirred at RT overnight. If starting material remained, the reaction mixture was stirred at 40 ^{o}C overnight.
Method B: A solution of compound **11** (100 mg, 1.1mmol) in CH_2Cl_2 (10mL) was treated with TEA (162 μL, 1.2mmol, 1.2 equv.) and chloroacetyl chloride (102 μL, 1.2 mmol). The reaction mixture was stirred at room temperature overnight.
After reaction complete, the reaction mixture was purified by flash column chromatography (ethyl acetate:hexan=1:3) to give compound **12**.[13]
A solution of carbazole (20 mg, 0.12 mmol) in DMF (3 mL) was treated with NaH (6 mg, 0.24mmol, 2.0 equiv.). The reaction mixture was stirred at room temperature for 1hr and followed by compound **12** (20 mg, 0.12 mmol, 1.0 equiv.) in DMF (2mL). The reaction was stirred at 60 ^{o}C overnight. The reaction mixture was diluted with ethyl acetate (20mL) and wash with water. The organic layer was dried with Na_2SO_4, filtered, concentrated under reduce pressure. Crude material was purified by flash column chromatography (ethyl aceate:hexane=1:2) to give compound **13**.

KL044

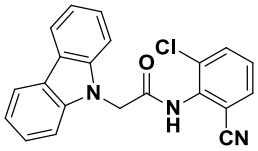

^{1}H NMR (**ACN-*d*, 400 MHz**) δ ; 8.5 (br s, 1H), 8.16 (d, J=7.6 Hz, 2H), 7.74 (dd, J=8, 1.2 Hz, 1H), 7.67 (dd, J=8, 1.6 Hz, 1H), 7.59 (d, J=8 Hz, 2H), 7.52 (t, J=8Hz, 2H), 7.41 (t, J=8 Hz, 1H), 7.29 (t, J=7.6 Hz, 2H), 5.25 (s, 2H).
^{13}C NMR (**ACN-*d*, 100 MHz**) δ ; 168.3, 144.6, 137.2, 135.2, 133.6, 132.7, 129.8, 126.9, 121.0, 120.6, 116.4, 115.1, 110.0, 47.0.
ESI-MS ; 360.0 (M+H).

KL046

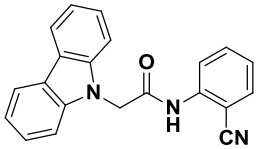

^{1}H-NMR (**$CDCl_3$-*d*, 400 MHz**) δ ; 8.21 (d, J=8.4Hz, 1H), 8.16 (d, J=7.6Hz, 2H), 7.73 (s, 1H), 7.56-7.51 (m, 3H), 7.46-7.41 (m, 3H), 7.35 (t, J=8 Hz, 2H), 7.14 (t, J=7.6 Hz, 1H), 5.13 (s, 2H).
^{13}C NMR (**$CDCl_3$-*d*, 100 MHz**) δ ; 166.9, 140.0, 138.9, 133.9, 132.3, 126.7, 125.8, 123.9, 122.0, 121.0, 120.3, 119.4, 110.6, 108.4, 47.6.
ESI-MS : 326.1 (M+H), 348.1 (M+Na).

KL047

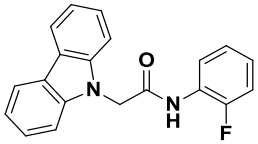

^{1}H-NMR (**$CDCl_3$-*d*, 400 MHz**) δ ; 8.20 (d, J=7.6 Hz, 1H), 8.15 (d, J=7.6 Hz, 2H), 7.526 (t, J=8 Hz, 2H), 7.43 (d, J=8 Hz, 2H), 7.35 (t, J=7.6 Hz, 2H), 7.08 (t, J=7.2 Hz, 1H), 7.05-6.97 (m, 1H), 6.94-6.86 (m, 1H), 5.09 (s, 2H).
ESI-MS : 319.1 (M+H), 341.1 (M+Na).

KL048

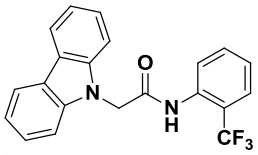

^{1}H NMR (**$CDCl_3$-*d*, 400 MHz**) δ ; 8.19 (d, J=8 Hz, 1H), 8.15 (d, J=7.6, 2H), 7.58 (s, 1H), 7.52 (t, J=8, 3H), 7.42 (d, J=8 Hz, 3H), 7.34 (t, J=8 Hz, 2H), 7.17 (m, 1H), 5.11 (s, 2H).
^{13}C NMR (**$CDCl_3$-*d*, 100 MHz**) δ ; 167.0, 140.0, 132.8, 130.1, 126.6, 125.0, 124.3, 123.7, 120.8, 120.7, 108.4, 47.6.
ESI-MS : 369.1 (M+H), 391.1 (M+Na).

KL049

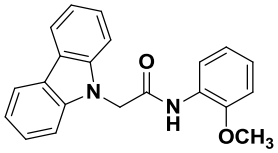

^{1}H NMR (**$CDCl_3$-*d*, 400 MHz**) δ ; 8.26 (dd, J=7.6, 1.2 Hz, 1H), 8.16 (d, J=8 Hz, 2H), 7.81 (s 1H), 7.51 (t, J=7.2 Hz, 2H), 7.44 (d, J=8.4 Hz, 2H), 7.33 (t, J=7.2 Hz, 2H), 7.0-6.87 (m, 2H). 6.62 (dd, J=8, 1.2 Hz, 1H), 5.09 (s, 2H), 3.22 (s, 3H).
^{13}C NMR (**$CDCl_3$-*d*, 100 MHz**) δ ; 165.8, 148.0, 140.2, 132.5, 126.4, 124.4, 123.6, 121.0, 120.6, 120.3, 119.8, 110.2, 108.8, 55.4, 47.7.
ESI-MS : 331.1 (M+H), 353.1 (M+Na).

KL050

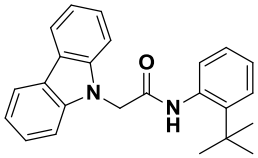

^{1}H-NMR (**$CDCl_3$-*d*, 400 MHz**) δ ; 8.13 (d, J=7.6 Hz, 2H), 7.84 (dd, J=8.4, 1.2 Hz, 1H), 7.52 (t, J=8 Hz, 2H), 7.47 (d, J=8 Hz, 2H), 7.32 (d, J=8 Hz, 3H), 7.23-7.17 (m, 2H), 7.06 (t, J=7.6 Hz, 1H), 5.14 (s, 2H), 0.69 (s, 9H).
ESI-MS : 357.2 (M+H), 379.1 (M+Na).

KL051

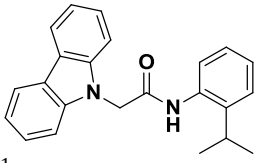

^{1}H-NMR (**$CDCl_3$-*d*, 400 MHz**) δ ; 8.15 (d, J=7.6 Hz, 2H), 7.78 (d, J=7.6 Hz, 1H), 7.53 (t, J=8 Hz, 2H), 7.47 (d, J=8 Hz, 2H), 7.34 (t, J=8 Hz, 2H), 7.14 (m, 1H), 7.10-7.03 (m, 2H), 7.0 (s, 1H), 5.14 (s, 2H), 1.87 (ddd, J=20.4, 13.6, 6.8 Hz, 1H), 0.62 (d, J=6.8 Hz, 6H).
ESI-MS 343.1 (M+H), 365.1 (M+Na).

KL055

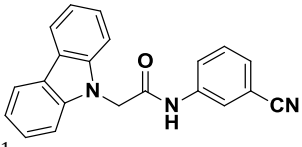

^{1}H-NMR (**$CDCl_3$-*d*, 400 MHz**) δ ; 8.17 (d, J=8Hz, 2H), 7.75 (br s, 1H), 7.54 (t, J=8, 1.2 Hz, 2H), 7.43-7.38 (m, 4H), 7.37-7.28 (m,4H), 5.07 (s, 2H).

KL056

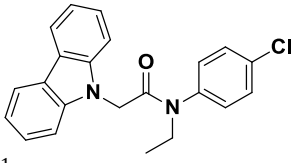

^{1}H-NMR (**$CDCl_3$-*d*, 400 MHz**) δ ; 8.01 (d, J=7.6 Hz, 2H), 7.37 (t, J= 8Hz, 2H), 7.23-7.15 (m, 4H), 7.11 (d, J=8.4 Hz, 2H), 6.88 (d, J=8.4 Hz, 2H), 4.81 (s, 2H), 3.69 (q, J=7.2 Hz, 2H), 1.086 (t, J=7.2 Hz, 3H).
ESI-MS : 363.1 (M+H), 385.1 (M+Na).

KL057

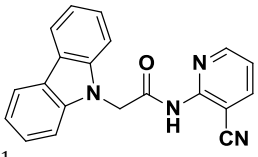

^{1}H-NMR (**$CDCl_3$-*d*, 400 MHz**) δ ; 8.13-8.11 (m, 3H), 7.58-7.47 (m, 3H), 7.42-7.34 (m, 3H), 7.31-7.27 (m, 2H), 5.06 (s, 2H).
ESI-MS : 327.1 (M+H), 349.1 (M+Na).

KL060

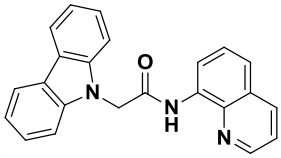

^{1}H-NMR (**$CDCl_3$-*d*, 400 MHz**) δ ; 10.05 (s, 1H), 8.70 (dd, J=7.2, 1.6 Hz, 1H), 8.20-8.17 (m, 3H), 7.99 (dd, J=8, 1.6 Hz, 1H), 7.52-7.41 (m, 5H), 7.33 (m, 2H), 7.22 (dd, J=8.4, 4.4 Hz, 1H), 5.21 (s, 2H).

ESI-MS : 352.1 (M+H), 374.1 (M+Na).

KL062

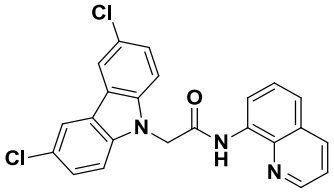

^{1}H NMR (**$CDCl_3$-*d*, 400 MHz**) δ ; 9.95 (s, 1H), 8.66 (dd, J=6.4, 2.8 Hz, 1H), 8.28 (dd, J=4, 1.6 Hz, 1H), 8.09 (dd, J=2, 0.4 Hz, 2H), 8.04 (dd, J=8.4, 1.6 Hz, 1H), 7.48-7.45 (m, 4H), 7.40 (d, J=8.4 Hz, 2H), 7.30-7.28 (m,1H), 5.18 (s, 2H).
ESI-MS : 420.1 (M+H).

KL065

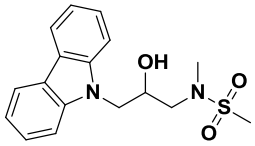

^{1}H-NMR (**$CDCl_3$-*d*, 400 MHz**) δ ; 8.09 (br d, J=8 Hz, 2H), 7.50-7.42 (m, 4H), 7.26 (td, J=8.0, 2.0 Hz, 2H), 4.38 (s, 3H), 3.38 (dd, J=14.4, 7.2 Hz, 1H), 3.20 (dd, J=14.4, 3.6 Hz, 1H), 2.88 (s, 3H), 2.81 (s, 3H).
^{13}C-NMR (**$CDCl_3$-*d*, 100 MHz**) δ ; 140.7, 126.0, 123.1, 120.4, 119.5, 108.9, 69.0, 54.1, 47.1, 36.4, 35.5.

KL067

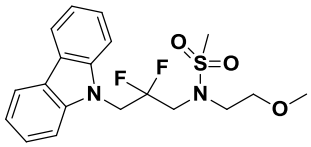

^{1}H NMR (**$CDCl_3$-*d*, 400 MHz**) δ ; 8.09 (d, J=8.0 Hz, 2H), 7.48 (t, J=8.0, 8.4 Hz, 2H), 7.41 (d, J=8.4 Hz, 2H), 7.30-7.25 (m, 2H), 4.74 (t, J=15.2 Hz, 2H), 3.93 (t, J=14.4 Hz, 2H), 3.62 (t, J=5.2, 2H), 3.56 (t, J=4.8 Hz, 2H).3.25 (s, 3H), 3.01 (s, 3H).

SI Table

Table S1. The structure of training set (black), test set (blue), and prediction set (red) compounds with experimental and predicted activities. NA: not active.

ID	pEC_{50} experiment (predicted)	Structure
KL001	6.16 (5.9)	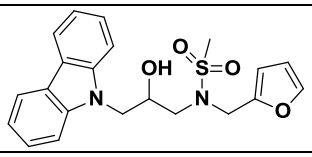
KL002	5.83 (5.8)	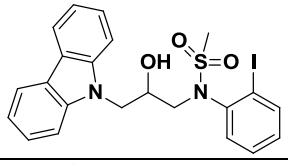
KL004	4.60 (4.8)	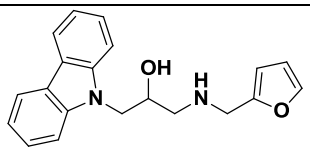
KL005	NA	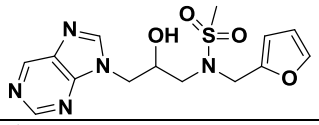
KL006	NA	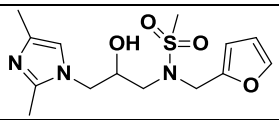
KL007	3.94 (3.9)	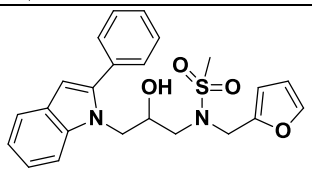
KL008	4.36 (4.2)	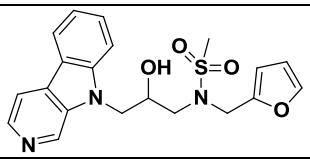
KL009	5.89 (5.5)	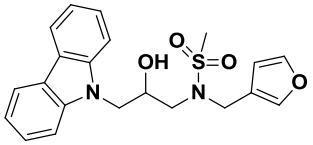
KL010	4.48 (4.8)	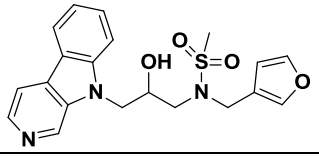

KL011	4.82 (4.6)	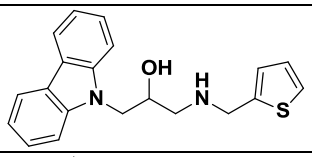
KL012	5.16 (5.1)	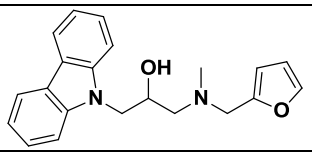
KL013	5.57 (5.5)	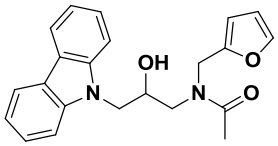
KL014	5.71 (5.3)	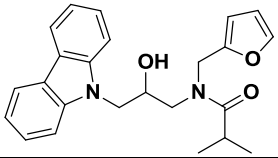
KL015	5.31 (5.5)	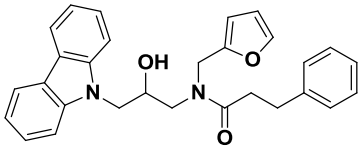
KL016	4.73 (4.8)	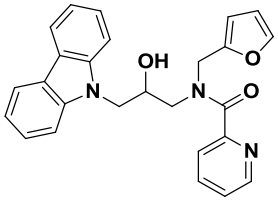
KL017	4.50 (4.6)	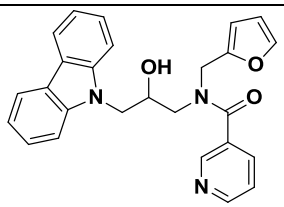
KL018	5.42 (5.1)	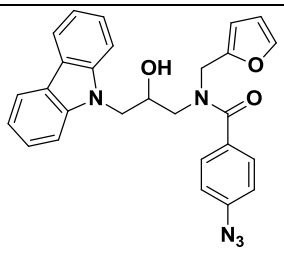
KL019	5.61 (5.5)	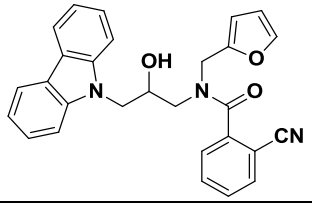

KL020	5.62 (5.5)	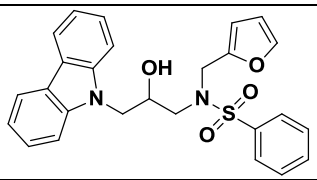
KL021	5.49 (5.5)	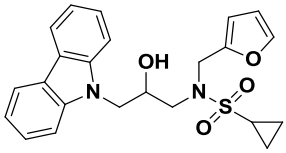
KL022	5.70 (5.8)	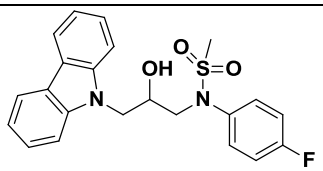
KL023	5.57 (5.5)	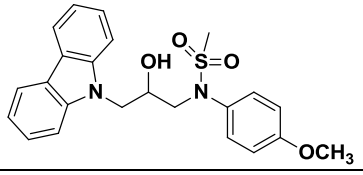
KL024	4.89 (5.1)	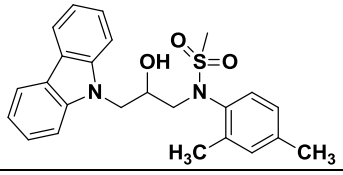
KL025	5.39 (5.4)	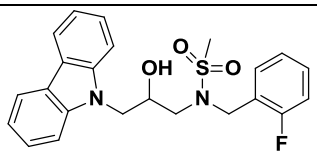
KL026	5.21 (5.1)	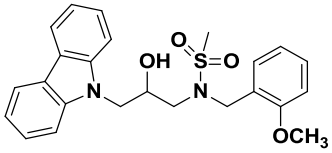
KL027	4.99 (5.0)	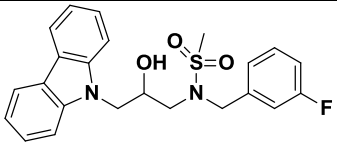
KL028	4.94 (5.0)	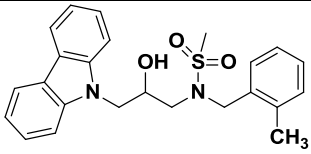
KL029	4.94 (4.9)	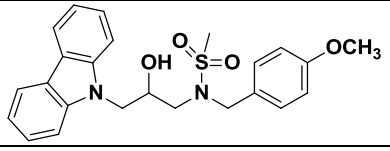

KL030	4.77 (4.8)	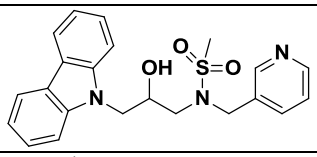
KL031	5.86 (5.9)	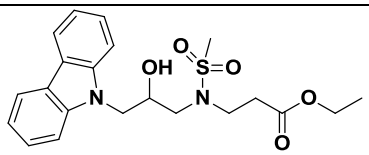
KL032	4.25 (4.4)	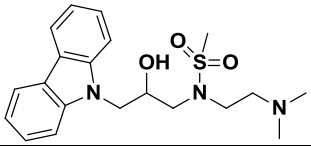
KL033	4.23 (4.3)	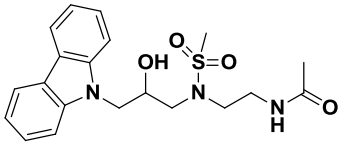
KL034	6.01 (5.9)	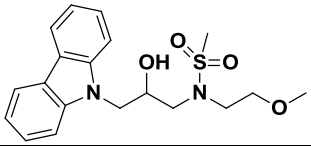
KL035	5.81 (5.9)	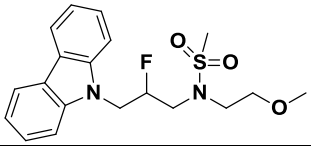
KL036	5.33 (5.5)	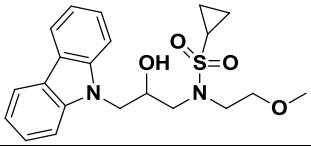
KL037	4.88 (4.9)	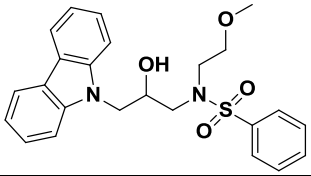
KL038	4.44 (4.4)	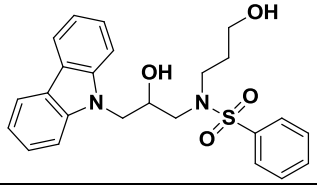
KL039	4.49 (4.5)	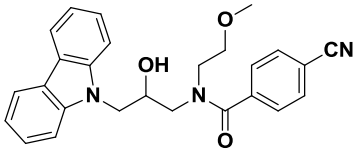
KL040	4.45 (4.5)	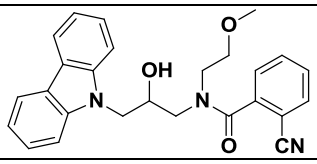

KL041	4.20 (4.3)	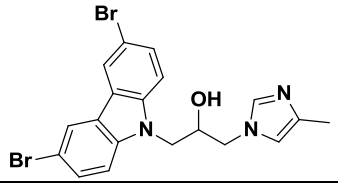
KL042	5.03 (5.0)	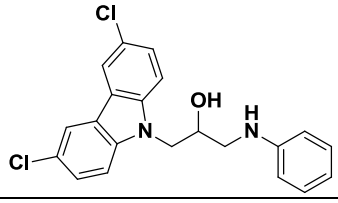
KL043	6.44 (6.3)	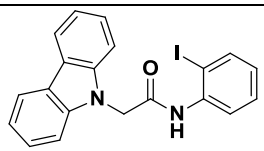
KL044	7.32 (7.3)	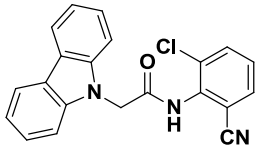
KL045	4.23 (4.2)	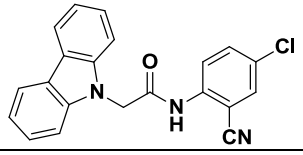
KL046	6.46 (6.2)	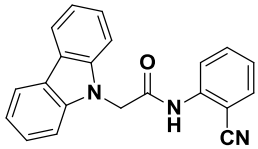
KL047	5.49 (5.6)	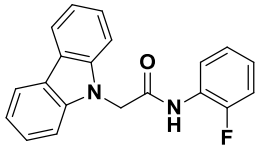
KL048	6.12 (6.0)	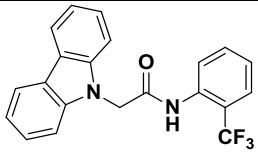
KL049	5.91 (5.8)	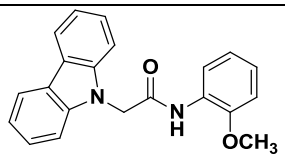
KL050	5.55 (5.6)	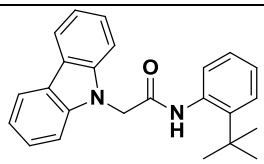

KL051	5.47 (6.0)	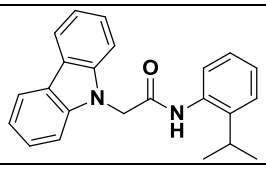
KL052	5.37 (5.3)	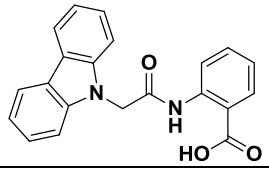
KL053	6.27 (6.3)	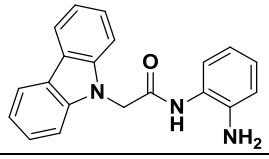
KL054	4.86 (4.9)	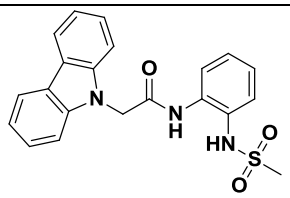
KL055	NA	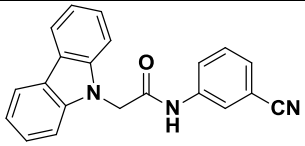
KL056	4.89 (4.8)	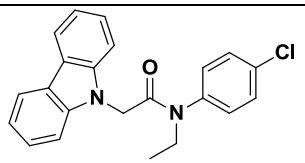
KL057	4.73 (4.6)	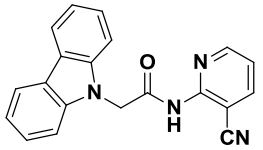
KL058	4.09 (4.0)	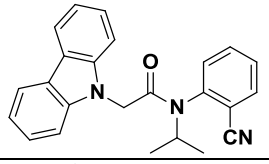
KL059	3.97 (4.0)	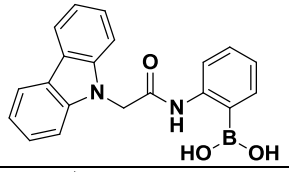
KL060	5.69 (5.7)	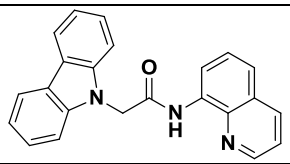

KL061	4.47 (4.5)	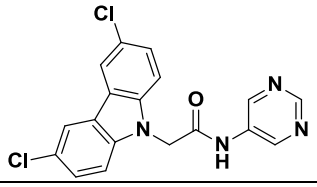
KL062	4.12 (4.1)	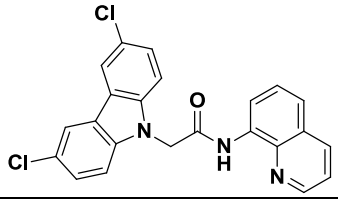
KL063	6.18 (5.8)	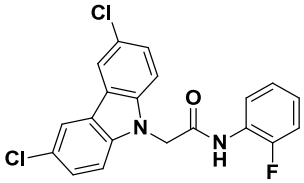
KL064	4.14 (4.1)	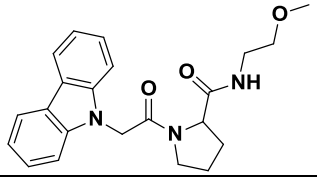
KL065	6.18 (5.9)	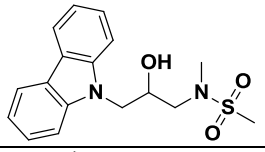
KL066	6.14 (6.1)	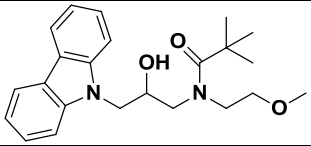
KL067	4.54 (5.1)	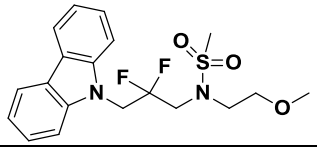
KL068	4.16 (5.1)	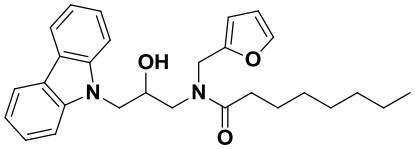
KL069	3.83 (4.3)	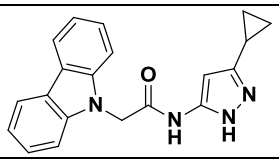

SI Figures

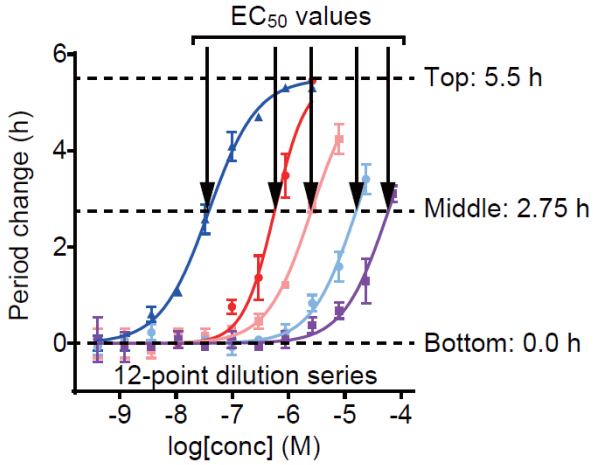

Figure S1: Determination of EC_{50} values of period lengthening effects of KL001 derivatives in *Bmal1-dLuc* reporter cells.

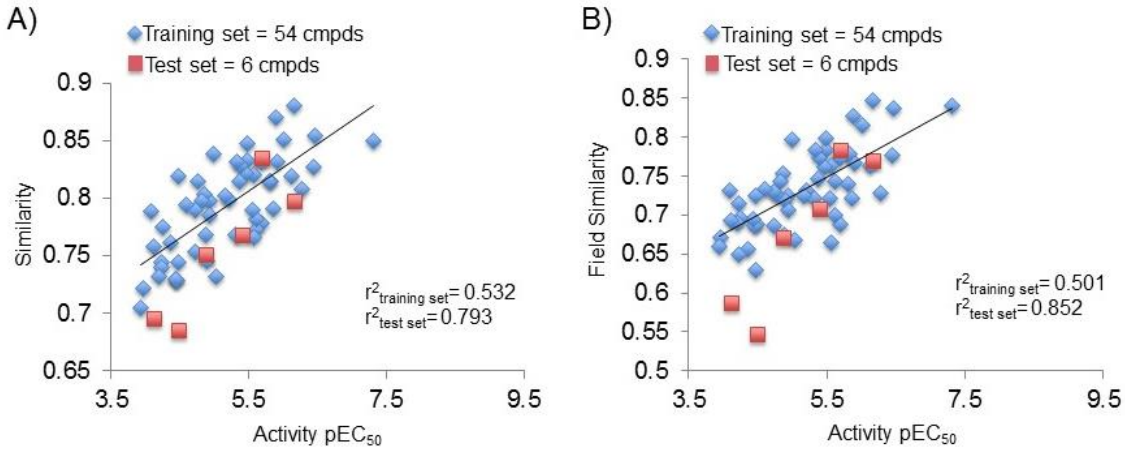

Figure S2. Plot of Field Similarity and experimental pEC_{50} values for 54 training compounds (blue) and 6 test set compounds (red).

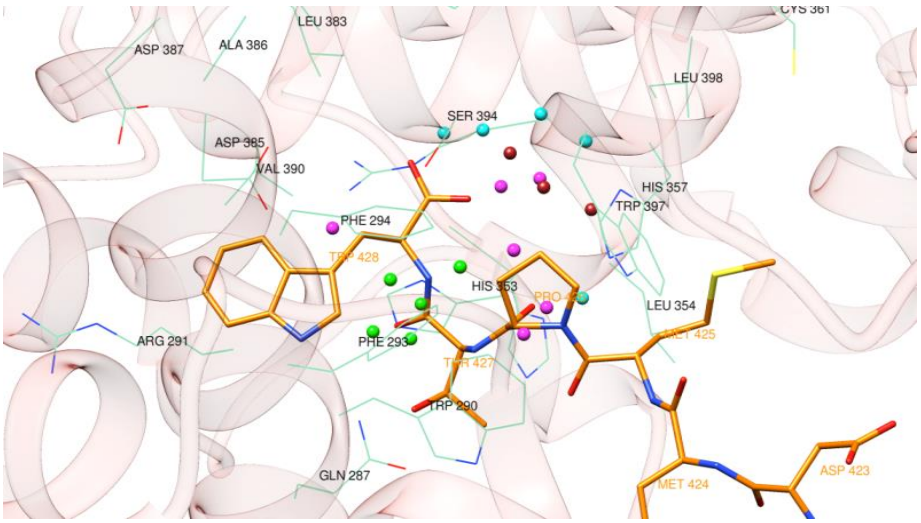

Figure S3. Overlaid pose of QSAR field points with CRY (PDB ID: 4MLP) and FBXL3 (PDB ID: 4I6J).

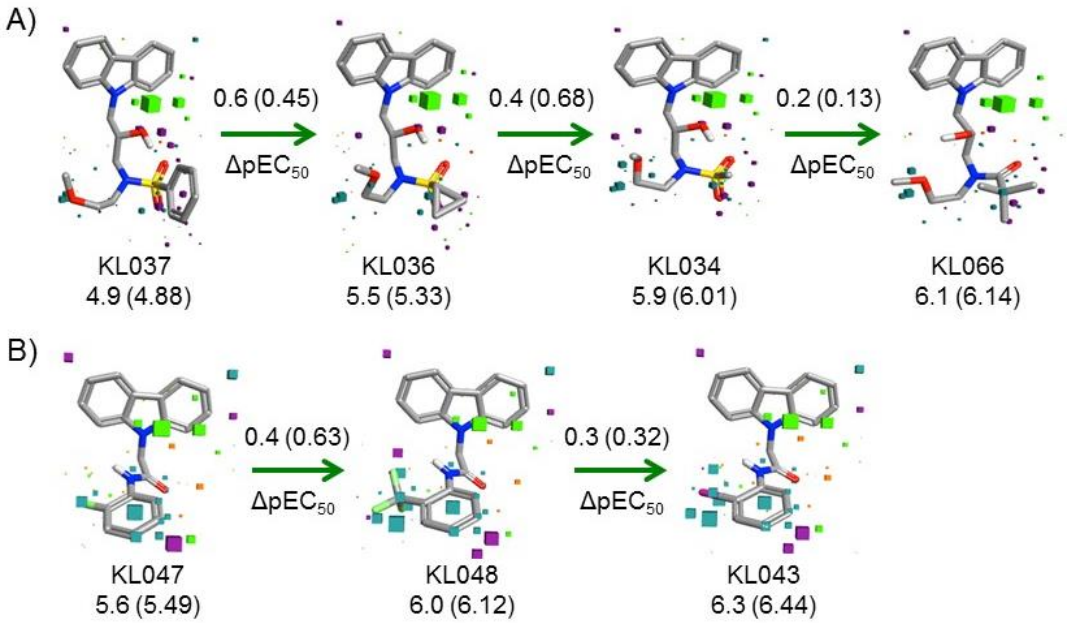

Figure S4. Comparison of A) the predicted compound KL066 in KL001 series and B) substituent at ortho benzyl moiety in KL044 series based on the contribution of the field points to the predicted activity in 3D-QSAR. Experimental pEC_{50}s are given in the brackets. Color code for field points contributions: favorable electrostatic (green), unfavorable electrostatic (orange), favorable steric (cyan), and unfavorable steric (purple).

SI References

1. Hirota, T., Lee, J. W., St. John, P. C., Sawa, M., Iwaisko, K., Noguchi, T., Pongsawakul, P. Y., Sonntag, T. Welsh, D., Brenner, D. A., Doyle III, F. J., Schultz, P. G., Kay, S. A., Identification of small molecule activators of cryptochrome. *Science* **2012**, 337, 1094-1097.
2. Torch, Cresset BioMolecular Discovery Ltd., **2014**.
3. a) Hunter, C. A.; Sanders, J. K. M., The nature of .pi.-.pi. interactions. *J. Am. Chem. Soc*. **1990**, 112, 5525-5534; b) Vinter, J. G., Extended electron distributions applied to the molecular mechanics of some intermolecular interactions. *J. Comput.-Aided Mol. Des.* **1994**, *8*, 653-668; c) Vinter, J. G., Extended electron distributions applied to the molecular mechanics of some intermolecular interactions. II. Organic complexes. *J. Comput.-Aided Mol. Des.* **1996**, 10, 417-426.
4. Pettersen, E. F.; Goddard, T. D.; Huang, C. C.; Couch, G. S.; Greenblatt, D. M.; Meng, E. C.; Ferrin, T. E., UCSF Chimera-A visualization system for exploratory research and analysis. *J Comput. Chem.* **2004**, 25, 1605-1612.
5. Nagle, S., Xing, W., Zheng, N., Crystal structure of mammalian cryptochrome in complex with a small molecule competitor of its ubiquitin ligase. *Cell Res.* **2013**, 23, 1417-1419.
6. Dunbrack Jr. R. L., Rotamer Libraries in the 21st Century. *Curr. Opin. Struct. Biol.* **2002**, 12, 431-440.
7. Wang, J., Wang, W., Kollman, P. A., Case, D. A., ANTECHAMBER. *J. Mol. Graph and Model* **2006**, 25, 247-260.
8. Morris, G. M., Huey, R., Lindstrom, W., Sanner, M. F., Belew, R. K., Goodsell, D. S., Olson, A. J., Autodock4 and AutoDockTools4: automated docking with selective receptor flexiblity. *J. Comput. Chem.* **2009**, 16, 2785-2791.
9. Forge, Cresset BioMolecular Discovery Ltd., **2014**.
10. Cheeseright, T., Mackey, M., Rose, S., Vinter, A., Molecular Field Extrema as Descriptors of Biological Activity: Definition and Validation. *J. Chem. Inf. Model.* **2006**, 46, 665-676.
11. Low, C. M., Vinter, J. G., Rationalizing the activities of diverse cholecystokinin 2 receptor antagonists using molecular field points. *J. Med. Chem.* **2008**, 51, 565–573.
12. Collins, J. C., Armstrong, A., Chapman, K. L., Cordingley, H. C., Jaxa-Chamiec, A. A., Judd, K. E., Mann, D. J., Scott, K. A., Tralau-Stewart, C. J., Low, C. M. R., Prospective use of molecular field points in ligand-based virtual screening: efficient identification of new reversible Cdc25 inhibitors. *Med. Chem. Commun.*, **2013**, 4, 1148-1155.
13. Guo, X., Ma, X., Yang, Q., Xu, J., Huang, L., Jia, J., Shan, J., Liu, L., Chen, W., Chu, H., Wei, J., Zhang, X., Sun, H., Tang, Y., You, Q., Discovery of 1-aryloxyethyl piperazine derivatives as Kv1.5 potassium channel inhibitors (part I). *Eur. J. Med. Chem.* **2014**, *81*, 89-94.